J Therm Anal Calorim (2016) 123:583–594
DOI 10.1007/s10973-015-4975-4

Novel synthesis of 2-imino-2*H*-chromene-3-carboximide metal complexes

Thermal decomposition, spectral studies and antimicrobial activity evaluation

Madiha H. Soliman[1] · Gehad G. Mohamed[2] · Galal H. Elgemeie[1]

Received: 19 May 2015 / Accepted: 6 August 2015 / Published online: 4 September 2015

Abstract New metal complexes derived from the reaction of Cr(III), Mn(II), Fe(III), Co(II), Ni(II), Cu(II) and Zn(II) chlorides with the 2-imino-2*H*-chromene-3-carboximide organic ligand (HL) have been synthesized. The resulting complexes have been characterized by elemental analysis (CHN), IR, magnetic susceptibility, mass spectra, ^{1}HNMR, UV–Vis, ESR, thermal analysis (TG, DTG and DTA) and molar conductance measurements. All the complexes are 1:2 and 1:3 electrolytes according to their molar conductivities. The microanalyses and spectroscopic data showed that the metal(II)/(III) ions in these complexes achieved coordination number of six and hence have octahedral geometrical structures. This is attained by bonding to the bidentate ligand via its two amino nitrogen atoms and two imine nitrogen atoms, and two monodentate aquo groups via its oxygen atoms. The results showed that the ligand acts as neutral bidentate coordinating via amino and NH nitrogens without displacement of hydrogen. The antimicrobial activities of the chromene ligand and its complexes have been tested against a number of pathogenic bacteria and fungi to assess their inhibiting potential. Antimicrobial studies indicate that these complexes exhibit better activity than the chromene ligand.

Graphical abstract

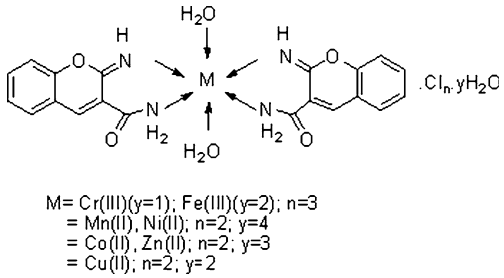

Keywords Coumarin · Metal complexes · IR · Thermal analysis · Mass spectra · Antimicrobial activity

Introduction

The fusion of α-pyrone ring with benzene nucleus gives rise to a class of heterocyclic compounds known as coumarin (benzo-α-pyrones). Except for coumarin and dicoumarol, all other naturally occurring coumarins are derivatives of 7-hydroxy-coumarin. Natural and synthetic coumarin derivatives represent, nowadays, an important group of organic compounds that are used as antibiotics [1, 2], fungicides [3], anti-inflammatory [4], anticoagulant [5] and antitumor agents [6, 7]. Regarding their high fluorescence ability, they are widely used as optical whitening agents, brighteners, laser dyes and also as fluorescent probes [8–10] in biology and medicine [11].

Hydroxycoumarins find wide applications as analytical reagents in the determination of metal ions [12–15]. The crystal structure of our *N*-(4-halophen-yl)-4-oxo-4H-chromene-3-carboxamides (halo = F, Cl, Br and I), *N*-(4-fluorophen-yl)-4-oxo-4H-chromene-3-carboxamide, $C_{16}H_{10}FNO_3$,

✉ Madiha H. Soliman
drmadihahasn@yahoo.com

[1] Chemistry Department, Faculty of Science, Helwan University, P.O. Box 11795, Helwan, Egypt

[2] Chemistry Department, Faculty of Science, Cairo University, Giza 12613, Egypt

N-(4-chloro-phen-yl)-4-oxo-4H-chromene-3-carboxamide, $C_{16}H_{10}ClNO_3$, *N*-(4-bromo-phen-yl)-4-oxo-4H-chromene-3-carboxamide, $C_{16}H_{10}BrNO_3$, and *N*-(4-iodo-phen-yl)-4-oxo-4H-chromene-3-carboxamide, $C_{16}H_{10}INO_3$, has been characterized [16].

Spectroscopic studies involving mixed ligand complexes of coumarilic acid/nicotinamide with transition metal complexes have been reported [17]. The present work aims to describe the coordination behavior of novel complexes of 2-imino-2*H*-chromene-3-carboxamide toward some bi- and trivalent transition metal ions like Cr(III), Mn(II), Fe(III), Co(II), Ni(II), Cu(II) and Zn(II). The structure of the synthesized complexes is elucidated using elemental analysis, IR, XRD, magnetic moment, molar conductance and thermal analysis measurements. The antimicrobial activities of the ligand and its metal complexes were detected on gram-positive and gram-negative bacteria and on fungi organisms. The antimicrobial activity of the ligand and its metal complexes is reported.

Experimental

Material and reagents

All chemicals used were of the analytical reagent grade (AR) and of the highest purity available. They included $CuCl_2{\cdot}2H_2O$, $NiCl_2{\cdot}6H_2O$, $MnCl_2$, $CoCl_2{\cdot}6H_2O$ and $CrCl_3{\cdot}6H_2O$. They were supplied from Sigma. $ZnCl_2{\cdot}2H_2O$ (Ubichem) and $FeCl_3{\cdot}6H_2O$ (Prolabo) were also used. Organic solvents included absolute ethyl alcohol, diethyl ether, dimethylformamide (DMF) and acetone. They were spectroscopically pure from BDH. Hydrogen peroxide, hydrochloric and nitric acids (Merck), cyanoacetamide (Sigma), salicyladehyde (Aldrich), ammonium acetate (Fluka), tryptone (Oxford), yeast extract (Oxford) and agar (Adwic) were also used. Deionized water collected from all glass equipments was usually used in all preparations.

Solutions

Stock solutions of the chromene ligand and its metal complexes (1.0×10^{-3} M) were prepared by dissolving the accurately weighed amount in DMF. Dilute solutions of the chromene ligand (1×10^{-5} M) and its metal complexes (1×10^{-4} M) were prepared by accurate dilution of the previous prepared stock solution.

Instruments

The molar conductance of solid chelates in DMF was measured using Sybron-Barnstead conductometer (Meter-PM. 6, $E = 3406$). Elemental microanalyses of the solid chelates for C, H and N were performed at the Microanalytical Center, Cairo University. The analyses were repeated twice to check the accuracy of the analyzed data. The X-ray powder diffraction analyses were carried out by using Philips Analytical X-ray BV, diffractometer type PW 1840. Radiation was provided by copper target (Cu anode 2000 W) high-intensity X-ray tube operated at 40 kV and 25 mA. Divergence and the receiving slits were 1 and 0.2, respectively. Infrared spectra were recorded on Perkin-Elmer FTIR type 1650 spectrometer in wave number region 4000–400 cm^{-1}. The spectra were recorded as KBr pellets. The solid reflectance spectra were measured on Shimadzu 3101 PC spectrophotometer. The magnetic susceptibility was measured on powdered samples using the Faraday method. The diamagnetic corrections were made by Pascal's constant, and $Hg[Co(SCN)_4]$ was used as a calibrant. The ^{1}HNMR spectra were recorded using 300 MHz Varian-Oxford Mercury. The deuterated solvent used was dimethylsulfoxide (DMSO-d_6), and the spectra extended from 0 to 15 ppm. The thermal analyses (TG, DTG and DTA) were carried out in dynamic nitrogen atmosphere (20 mL min^{-1}) with a heating rate of 10 °C min^{-1} using Shimadzu TG-60H and DTA-60H thermal analyzers. The electronic spectra were recorded in DMF at room temperature on Shimadzu UV–visible mini-1240 spectrophotometer. Electron spin resonance spectra were also recorded on JES-FE2XG ESR spectrophotometer at Microanalytical Center, Tanta University. Mass spectra were recorded by the EI technique at 70 eV using MS-5988 GS-MS Hewlett-Packard instrument at the Microanalytical Center, National Center for Research, Egypt.

Synthesis of the ligand HL

2-Imino-2*H*-chromene-3-carboximide ligand (HL) was prepared by the reaction of cyanoacetamide with salicyladehyde in ethanol/ammonium acetate mixture at 50 °C for 10 min [18]. The ligand has yellowish orange color with 85 % yield.

Synthesis of metal complexes

The chromene metal complexes were prepared by the addition of hot solution (50 °C) of the appropriate metal chloride (1.0 mmol) in an ethanol–water mixture (1:1, 25 mL) to hot solution (50 °C) of HL (0.3762 g HL, 2.0 mmol) in DMF (25 mL). The mixture was left on a steam bath for 30 min. In some cases, when the metal chelates did not separate on standing, drops of ammonia solution (1:10) were added slowly with stirring until pH 6–8 was attained, at which point the metal complexes separated. They were collected by filtration and purified by washing with an ethanol–water mixture (1:1). The

analytical data for C, H and N were repeated twice. The percent yield was ranged from 68 to 76 %.

Biological activity

The newly synthesized complexes were tested for their biological activity in vitro against bacteria strains such as *Escherichia coli*, *Staphylococcus aureus*, *Neisseria gonorrhoeae*, *Bacillus subtilis* and *Candida albicans* employing susceptibility test method. To a sterile agar medium, 0.5 mL spore suspension (10^{-7}–10^{-8} spore mL^{-1}) of each of the investigated organisms was added just before solidification, then poured into sterile petri dishes (9 cm in diameter) and left to solidify. Using sterile cork borer (6 mm in diameter), three holes (wells) were made in each dish and then 0.1 mL of the tested compounds dissolved in DMF (100 μg mL^{-1}) were poured into these holes. LB agar media, a suitable media for most bacteria and composed of sodium chloride (10 g L^{-1}), tryptone (10 g L^{-1}), yeast extract (10 g L^{-1}) and agar (15 g L^{-1}), surface were inoculated with four investigated bacteria (two Gram–positive and two Gram–negative) and one fungi organism then transferred to a saturated disk with a tested solution in the center of petri dish (agar plates). Finally, the dishes were incubated at 37 °C for 48 h where clear or inhibition zones were detected around each hole. DMF (0.1 mL) alone was used as a control under the same condition for each organism, and by subtracting the diameter of inhibition zone resulting with DMF from that obtained in each case, both antibacterial and antifungal activities can be calculated as a mean of three replicates [19, 20].

Spectrophotometric studies

The absorption spectra were recorded for 1.0×10^{-5} M solutions of the chromene ligand and 10^{-4} M solutions of its metal complexes in DMF. The spectra were scanned within the wavelength range from 200 to 700 nm.

Results and discussion

The chromene ligand was prepared according to the previously published data [18] as given below (Eq. 1).

The physical and analytical data of the chromene ligand HL and its corresponding transition metal complexes are listed in Table 1. Cr(III), Ni(II), Cu(II) and Zn(II) complexes are brown, Mn(II) complex is yellowish brown, Fe(III) complex is deep red, while Co(II) complex is green in color. They are thermally stable above 300 °C. The results of elemental analyses (Table 1) suggest that the complexes are formed with 1:2 [metal]/[chromene] ratio, and they proposed to have the general formulae $[M(HL)_2(H_2O)_2]Cl_2{\cdot}nH_2O$ (M = Mn(II), Co(II), Ni(II), Cu(II) and Zn(II); n = 2–4) and $[M(HL)_2(H_2O)_2]Cl_3{\cdot}nH_2O$ (M = Cr(III) and Fe(III); n = 1–2). The complexes are insoluble in alcohols and most of the organic solvent, but they are soluble in dimethylformamide and dimethylsulfoxide.

Magnetic susceptibility and electronic spectra measurements

Magnetic moment values (Table 1) along with electronic spectral data were used to determine the stereochemistry of the isolated complexes. The room-temperature magnetic moments of all the complexes are in agreement with the spin-free values. The magnetic moment values for Cr(III), Mn(II), Fe(III), Co(II), Ni(II) and Cu(II) indicate the high-spin octahedral nature of the complexes (Table 1).

Hexa-coordinated Cr(III) complexes with octahedral symmetry showed three spin-allowed bands in the range of 18,000–30,000 cm^{-1}, while the complex under study showed four bands at 16,450, 25,050, 26,980 and 37,650 cm^{-1}, respectively, which may be assigned to $^4A_{2g}(F) \rightarrow {}^4T_{2g}(F)$, $^4A_{2g}(F) \rightarrow {}^4T_{1g}(F)$, $^4A_{2g}(F) \rightarrow {}^4T_{1g}(P)$ and $^4B_{1g} \rightarrow {}^4A_{1g}(\nu_4)$ transitions, respectively, expected for high-spin octahedral Cr(III) complexes [21–24].

The diffused reflectance spectrum of the Mn(II) complex exhibits three bands at 16,765, 20,080 and 25,640 cm^{-1} assignable to $^4T_{1g} \rightarrow {}^6A_{1g}$, $^4T_{2g}(G) \rightarrow {}^6A_{1g}$ and $^4T_{1g}(D) \rightarrow {}^6A_{1g}$ transitions, respectively [25–27], which indicated that the Mn(II) complex had octahedral geometry. The Fe(III) chelate exhibited bands from diffused reflectance spectrum at 21,240 cm^{-1}, which may be assigned to the $^6A_{1g} \rightarrow T_{2g}(G)$ transition in octahedral geometry of the complex [28, 29]. The two bands at 16,030 and 13,855 cm^{-1} resulted from the splitting of the $^6A_{1g} \rightarrow {}^5T_1g$ transition.

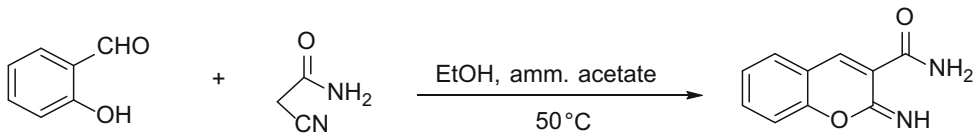

salicyladehyde cyanoacetamide chromene (1)

Table 1 Analytical and physical data of chromene ligand and its metal complexes

Compound/chemical formula	Color/%yield	MP/°C	Found/calcd. %					μ_{eff}/B.M.	$\Lambda m/\Omega^{-1}$ mol^{-1} cm^2
			C	H	N	Cl	M		
HL, $C_{10}H_8N_2O_2$	Yellowish orange (85)	178	63.62 (63.83)	4.05 (4.26)	15.22 (14.89)	–	–	–	–
$[Cr(HL)_2(H_2O)_2]Cl_3{\cdot}H_2O$ $C_{20}H_{22}CrCl_3N_4O_7$	Brown (75)	>300	40.35 (40.77)	3.86 (3.74)	9.64 (9.51)	18.25 (18.09)	9.12 (8.83)	5.05	182.0
$[Mn(HL)_2(H_2O)_2]Cl_2{\cdot}4H_2O$ $C_{20}H_{28}Cl_2MnN_4O_{10}$	Brownish yellow (72)	>300	40.67 (40.32)	4.81 (4.70)	9.63 (9.41)	11.63 (11.93)	8.87 (9.07)	4.99	118.5
$[Fe(HL)_2(H_2O)_2]Cl_3{\cdot}2H_2O$ $C_{20}H_{24}FeCl_3N_4O_8$	Deep red (76)	>300	39.02 (39.30)	3.84 (3.93)	9.35 (9.17)	16.99 (17.44)	9.05 (9.17)	5.45	178.0
$[Co(HL)_2(H_2O)_2]Cl_2{\cdot}3H_2O$ $C_{20}H_{24}Cl_2CoN_4O_8$	Green (70)	>300	40.6 (40.25)	4.15 (4.36)	9.80 (9.39)	11.52 (11.91)	9.42 (9.90)	5.08	124.3
$[Ni(HL)_2(H_2O)_2]Cl_2{\cdot}4H_2O$ $C_{20}H_{28}Cl_2NiN_4O_{10}$	Brown (71)	>300	39.07 (39.07)	5.00 (4.56)	9.05 (9.18)	11.33 (11.56)	9.24 (9.61)	3.55	148.0
$[Cu(HL)_2(H_2O)_2]Cl_2{\cdot}2H_2O$ $C_{20}H_{24}Cl_2CuN_4O_8$	Brown (74)	>300	40.88 (41.19)	4.41 (4.12)	9.36 (9.61)	12.66 (12.18)	10.60 (10.90)	1.88	127.5
$[Zn(HL)_2(H_2O)_2]$ $Cl_2{\cdot}3H_2O$ $C_{20}H_{26}Cl_2N_4O_9Zn$	Brown (68)	>300	40.43 (40.80)	4.41 (4.42)	9.02 (9.52)	12.42 (12.07)	11.29 (11.05)	Diam.	115.4

The diffused reflectance spectrum of Ni(II) complex showed the bands at 13,660, 16,380 and 26,555 cm^{-1} assignable to $^3A_{2g} \rightarrow {}^3T_{1g}$ (F), $^3A_{2g}(F) \rightarrow {}^3T_{2g}(F)$ and $^3A_{2g} \rightarrow {}^3T_{1g}$ (P) transitions, respectively, for an octahedral geometry [28, 30] around Ni(II) ion. The Co(II) complex exhibits three bands at 14,780, 17,690 and 22,698 cm^{-1} assignable to $^4T_{1g}(F) \rightarrow {}^4T_{2g}(F)$ (ν_1), $^4T_{1g}(F) \rightarrow {}^4A_{2g}(F)$ (ν_2) and $^4T_{1g}(F) \rightarrow {}^4T_{1g}(P)$ (ν_3) transitions, respectively, which suggested an octahedral geometry [28, 30–33] for the complex. The room-temperature magnetic moment values are summarized in Table 1. A magnetic moment value of 5.08 and 3.55 BM for Co(II) and Ni(II) complexes, respectively, is typical of octahedral environments around the metal centers [24, 31–34].

On the basis of diffused reflectance spectrum, distorted octahedral geometry around Cu(II) ion in complex is suggested [24, 35, 36]. The spectrum showed a broad band at 12,990 cm^{-1} (d_{x2-y2}/d_{xy} transition) and a second band at 17,480 cm^{-1} which may be assigned to $d_{x2-y2}/d_{xy;yz}$ transition. This complex had magnetic moment of 1.88 BM, which was expected for one unpaired electron and offered possibility of an octahedral geometry [24, 37–39].

The Zn(II) complex was diamagnetic as expected, and its geometry was most probably octahedral similar to the remaining complexes of the ligand under study.

Molar conductance measurements

The chelates were dissolved in DMF, and the molar conductivity of 10^{-3} M solutions is measured at room temperature (25 °C). Table 1 shows the molar conductance values of the complexes. It is concluded from the results that all the metal chelates had molar conductance values of 115.4–182.0 Ω^{-1} mol^{-1} cm^2 indicating their ionic nature and they behave as 1:2 (bivalent metal chelates) and 1:3 (trivalent metal chelates) electrolytes [40].

UV–Vis spectral studies

UV–Visible spectra of the chromene ligand (1×10^{-5} M) and its chelates (1×10^{-4} M) were carried out in DMF within the wavelength range from 200 to 700 nm at room temperature using the same solvent as blank. It can be seen that the chromene ligand has two sharp absorption bands. The first band at 294 nm may be attributed to π–π^* transition of the benzene ring. The second band observed at 348 nm can be attributed to n–π^* electronic transition. The spectra of metal complexes showed the π–π^* and n–π^* transition bands at 293–297 and 330–352 nm, respectively. The shift in the n–π^* transition band can be accounted to the participation of the lone pair of electrons on the amino group in binding to metal ions. The spectra of Cr(III), Co(II), Ni(II) and Cu(II) complexes showed a third

absorption band at 416, 418, 420 and 397 nm, respectively, which may be assigned to the charge transfer.

Powder X-ray diffraction spectroscopy

To obtain further evidence about the structure of the metal complexes, X-ray powder diffraction was performed. The diffractograms obtained for chromene organic ligand and its metal complexes were compared. The XRD patterns indicated crystalline nature of the complexes. It can also conclude that the pattern of the chromene organic ligand differs from its metal complexes, which may be attributed to the formation of a well-defined distorted crystalline structure. Probably, this behavior was due to the incorporation of water molecules into the coordination sphere.

Mass spectral studies

On the basis of earlier reported work, the ligand was characterized based on mass spectrometry. Molecular ion peak of ligand was observed at m/z = 188 with isotopic peak (almost 24 %) at m/z = 188. Base peak was observed at m/z = 143 with the cleavage of H_2O and HCN (path a), OC=NH (path b) or N_2 and ½O_2 (path c) groups from molecular ion. This molecular ion fragment was further disintegrated by the cleavage of CN group (path a) or C_2H_3 group (path c) resulting in the fragment peak at m/z = 118 (found 118, RI = 62 %). The fragment pattern of the molecules was observed also by the further cleavage and the resulting peak at m/z = 75 and followed by ring cleavage and so on (Scheme 1).

The proposed molecular formulae of $[Cr(HL)_2(H_2O)_2]Cl_3{\cdot}H_2O$, $[Fe(HL)_2(H_2O)_2]Cl_3{\cdot}2H_2O$ and $[Cu(HL)_2(H_2O)]Cl_2{\cdot}2H_2O$ metal complexes were confirmed by comparing their molecular formula weights with m/z values. The molecular ion peaks at m/z = 579 (RI = 1 %; M-½H_2O), 611 (RI = 1 %; M^+) and 582 amu (RI = 1 %; M^+) are the calculated molecular weights of 588.5, 610.5 and 582.5 g mol^{-1}, respectively. These data are in good agreement with the respective molecular formulae of metal complexes. The mass spectra of the complexes showed the parent HL ligand peak at 189 (RI = 23 %), 189 (RI = 8 %) and 189 amu (5 %) for Cr(III), Fe(III) and Cr(III) complexes, respectively, confirming the complex formation.

IR spectral studies

The most important IR bands are listed in Table 2. The bonding sites in the metal complexes were determined by a careful comparison of the spectra of the metal complexes and the spectrum of the chromene ligand [41]. The bands at 3056 cm^{-1} are assigned to ν(NH) of chromene organic moiety of the ligand. This band shifted to lower (3045–3050 cm^{-1}) or higher (3060–3075 cm^{-1}) wave number in the spectra of the complexes. This observation indicates that the NH group participates in complex formation.

The IR spectrum of the ligand showed the bands at 3289, 3217, 1613, 1546 and 755 cm^{-1} which are assigned to ν(NH_2) stretching, scissoring and in-plane and out-of-plane bending vibrations, respectively. These bands are shifted to higher or lower wave numbers in the spectra of metal complexes, confirming the binding of the chromene organic ligand to the metal ions with the amino nitrogen group. Therefore, the results indicated that the chromene ligand behaves as a neutral bidentate chelating ligand to the meal ions via the NH nitrogen and amino nitrogen without displacement of a hydrogen atom from the two groups (Table 2). The spectra also show bands in the region of 414–496 cm^{-1} assigned to ν(M–N) [42].

^{1}HNMR

The spectra of chromene ligand HL and its Zn(II) complex were recorded in d_6-dimethylsulfoxide (DMSO) solution using tetramethylsilan (TMS) as an internal standard.

The spectrum of the Zn(II) complex is examined in comparison with chromene HL ligand (Table 3). Upon examination, it was found that the analytical data for HL chromene ligand revealed a molecular formula $C_{10}H_8N_2O_2$. ^{1}HNMR spectra showed a multiplet at 6.66–8.99 and 6.70–8.90 ppm assigned to aromatic protons of chrome ligand and Zn(II) complex, respectively. A singlet bands at 4.60 and 11.10 and 4.52 and 11.0 ppm can be assigned to an amino (NH_2) and an imine NH protons in the chrome ligand and Zn(II) complex, respectively. The position of the amino NH_2 and imine NH protons is ascertained from the disappearance of these two bands upon addition of deuterated solvent. The shift in these two bands in the Zn(II) complex lower than that of the chromene ligand supported the participation of NH_2 and NH groups in chelation.

Thermal analyses (TG and DTG) studies

Table 4 shows the TG and DTG results of thermal decomposition of chromene (HL) ligand and its metal chelates. From these results, it was concluded that:

The chromene ligand decomposed in four steps within the temperature range from 30 to 700 °C. The first mass loss of 7.19 % (calcd. = 7.45 %) within the temperature range of 30–140 °C can be attributed to the loss of ½N_2 gas. The second step occurred within the temperature range of 140–370 °C (estimated mass loss = 35.86 %;

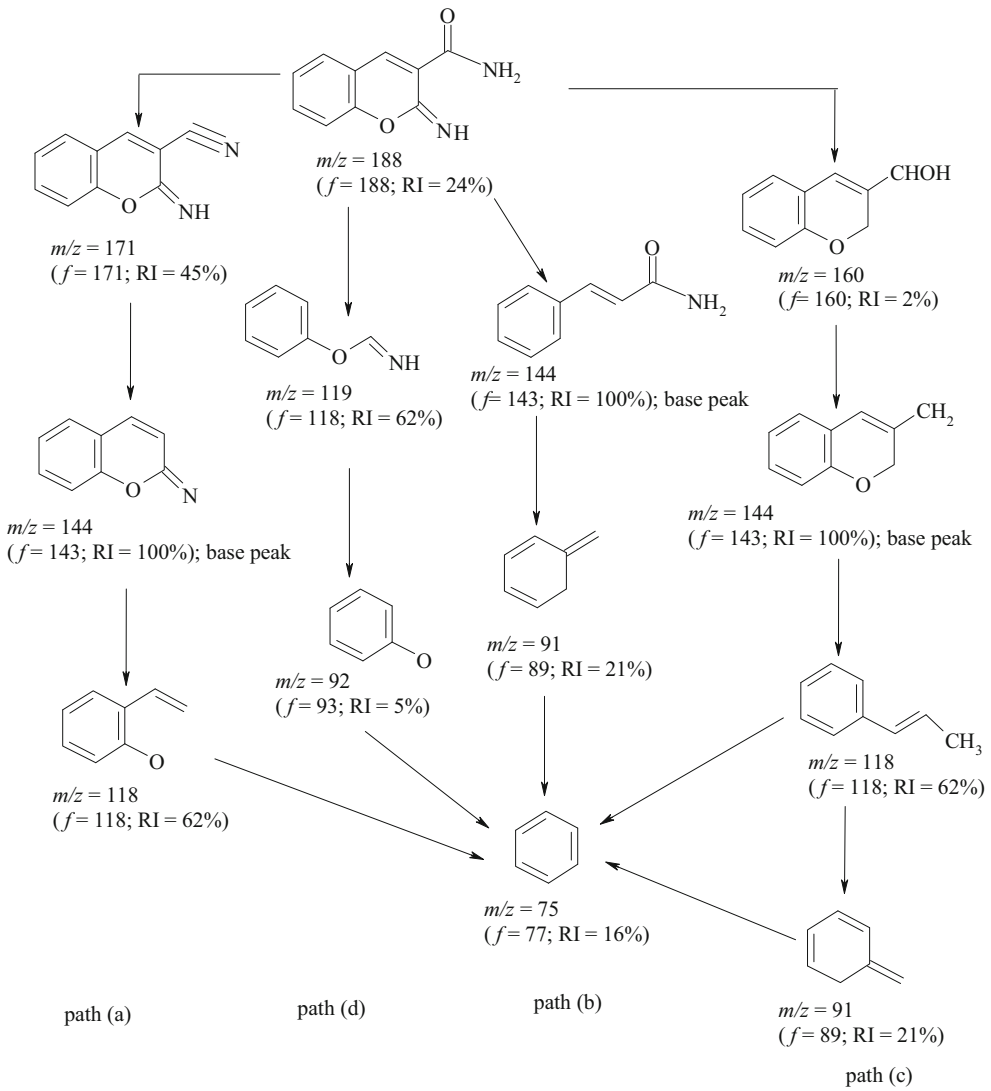

Scheme 1 Mass fragmentation pattern of chromene ligand

Table 2 IR spectra (4000–400 cm^{-1}) of chromene ligand and its binary metal complexes

Compound	$\nu(NH_2)$	$\nu(NH_2)$/scissoring	$\delta(NH_2)$/in plane	$\delta(NH_2)$/out of plane	ν(NH)	ν(C=O)	ν(M–N)
HL	3289m, 3217m	1613sh	1546m	755sh	3056m	1691sh	–
$[Cr(HL)_2(H_2O)_2]Cl_3{\cdot}H_2O$	3425–3300br	1648m	1535m	760sh	3047s	1719m	414s
$[Mn(HL)_2(H_2O)_2]Cl_2{\cdot}4H_2O$	3402–3320br	1624s	1530s	752s	3060w	1664sh	563s
$[Fe(HL)_2(H_2O)_2]Cl_3{\cdot}2H_2O$	3417–3147br	1648sh	1535m	759sh	3048m	1708m	496s
$[Co(HL)_2(H_2O)_2]Cl_2{\cdot}3H_2O$	3409–3200br	1653m	1527sh	755sh	3050s	1698m	415s
$[Ni(HL)_2(H_2O)_2]Cl_2{\cdot}4H_2O$	3384–3261br	1653m	1528sh	761sh	3045s	1703m	465s
$[Cu(HL)_2(H_2O)_2]Cl_2{\cdot}2H_2O$	3393–3132br	1656sh	1524sh	753sh	3046m	1696s	463s
$[Zn(HL)_2(H_2O)_2]\ Cl_2{\cdot}3H_2O$	3449–3280br	1654m	1525m	759sh	3075s	1705s	461s

sh sharp, *m* medium, *br* broad, *s* small, *w* weak

calcd. = 36.70 %) and can be accounted to the loss of C_3H_3NO molecule. The third step can be attributed to the loss of the remaining part of the chromene ligand with an estimated mass loss of 56.96 % (calcd. = 55.85 %) in the 370–700 °C temperature range. The DTA data are listed in Table 4. The decomposition of the chromene ligand

Table 3 ^{1}HNMR spectral data of chromene ligand and Zn(II) complex

Compound	Chemical shift (δ, ppm)	Assignment
HL	11.10	(s, 1H, =NH)
	6.66–8.99	(m, 5H, Ar–H)
	4.60	(s, 2H, NH_2)
$[Zn(HL)_2(H_2O)_2]Cl_2{\cdot}3H_2O$	11.00	(s, 2H, =NH)
	6.70–8.90	(m, 10H, Ar–H)
	4.60	(br, 4H, NH_2)

appeared in the DTA as endothermic (250, 313, 330 and 360 °C) and exothermic (233 and 300 °C) peaks.

The $[Cr(HL)_2(H_2O)_2]Cl_3{\cdot}H_2O$ chelate showed four stages of decomposition within the temperature range from 35 to 650 °C. The first step of decomposition at 35–110 °C temperature range can correspond to the loss of water molecules of hydration and Cl_2 gas. The DTA data listed in Table 4 showed that the Cr(III) complex had endothermic peak within this temperature of decomposition. The second stage occurred within the temperature range of 110–225 °C may be accounted for the loss of coordinated water and ½Cl_2 gas. This decomposition step appeared as endothermic peak at 160 °C in the DTA curve. While the subsequent steps involved loss of organic part of the chromene ligand molecules with an estimated mass loss of 60.42 % (calcd. = 59.83 %), these two decomposition steps are accompanied by endothermic and exothermic peaks in the DTA curve. The overall mass losses amount to 87.67 % (calcd. = 87.10 %), leaving chromium oxide as residue of decomposition. The two endothermic peaks observed at 700 and 800 °C can be attributed to phase change in the metal oxide residue.

The curves of $[Co(HL)_2(H_2O)_2]Cl_2{\cdot}3H_2O$ and $[Zn(HL)_2(H_2O)_2]Cl_2{\cdot}3H_2O$ chelates showed four stages of decomposition within the temperature range from 25 to 650 and 25 to 950 °C, respectively. The first stage corresponded to the loss of water molecule of hydration. The DTA data listed in Table 4 showed that the Zn(II) complex had endothermic peak at 60 °C, while Co(II) complex had endothermic and exothermic peaks within this temperature of decomposition (Table 4). The second step of decomposition can be attributed to the loss of coordinated water and ½Cl_2 in case of Co(II) complex and loss of coordinated water and 2 HCl molecules in case of Zn(II) complex. It is obvious from Table 4 that this decomposition step appeared in the DTA curves as endothermic and exothermic peaks for both complexes. While the subsequent steps involved loss of organic part of the chromene ligand molecules, these two steps are accompanied by the appearance of many endothermic and exothermic peaks within the temperature ranges given in Table 4. The overall mass losses amount to 80.49 % (calcd. = 79.12 %) and 85.87 % (calcd. = 86.45 %) for Co(II) and Zn(II) complexes, respectively.

The TG curves of $[Mn(HL)_2(H_2O)_2]Cl_2{\cdot}4H_2O$ and $[Fe(HL)_2(H_2O)_2]Cl_3{\cdot}2H_2O$ chelates exhibit three decomposition steps within the temperature range from 25 to 750 and 35 to 650 °C, respectively. The first step may be attributed to the loss of hydrated water and Cl_2 molecules (estimated mass loss = 23.86 % and calcd. = 24.03 %) and HCl and hydrated water (estimated mass loss = 64.99 %, calcd. = 64.21 %) within the temperature range from 25 to 130 and 35 to 140 °C for Mn(II) and Fe(III) chelates, respectively. The DTA data listed in Table 4 showed that the Mn(II) complex had two exothermic and one exothermic peaks, while Fe(III) complex had one endothermic and one exothermic peaks within the given decomposition temperature ranges. Meanwhile, the subsequent steps involved the loss of coordinated water and the organic part of the chromene ligand molecules in case of Mn(II) complex and Cl_2 and chromene organic part of the ligand in case of Fe(III) complex. These losses appeared as endothermic and exothermic peaks in the DTA curves of both complexes as given in Table 4. The overall mass losses amount to 88.85 % (calcd. = 88.24 %) and 84.56 % (calcd. = 84.61 %), leaving MnO and ½Fe_2O_3 as residues for Mn(II) and Fe(III) complexes, respectively.

On the other hand, $[Ni(HL)_2(H_2O)_2]Cl_2{\cdot}4H_2O$ and $[Cu(HL)_2(H_2O)_2]Cl_2{\cdot}2H_2O$ chelates exhibit five decomposition steps within the temperature range from 40 to 700 and 25 to 700 °C, respectively. The estimated mass losses within the temperature ranges given in Table 4 can be attributed to the loss of hydrated and coordinated water molecules, Cl_2, HCl and two chromene ligand molecules. According to the data listed in Table 3, the total mass losses of the decomposition steps were found to be 88.96 % (calcd = 87.79 %) and 85.48 % (calcd. = 83.96 %) for Ni(II) and Cu(II) complexes, respectively. The DTA data of both complexes are listed in Table 4. It is clear from these data that these decomposition steps appeared in the DTA curves as endothermic and exothermic peaks.

ESR spectra

The ESR spectrum of Cu(II) complex, recorded in the solid state, is consistent with the octahedral geometry around Cu(II) center in the complex [26, 31]. The ESR spectrum of Cu(II) complex gave an anisotropic signal with corresponding g-values as $g_{\parallel} = 2.284$ and $g_{\perp} = 2.065$. The trend in the observed "g" values $g_{\parallel} > g_{\perp} > g_e$ (2.0023) suggested that the unpaired electron lies mainly in the d_{x2-y2} orbital. For the reported Cu(II) complexes, $g_{\parallel} < 2.3$

Table 4 Thermoanalytical results (TG, DTG and DTA) of chromene ligand (HL) and its metal complexes

Complex	TG range/ °C	DTG_{max}/ °C	*n**	Mass loss % estim (calcd.)	Total mass loss %/%	Assignment	Metallic residue	DTA/°C
HL	35–140		1	7.19 (7.45)	100.01 (100.00)	Loss of 1/2 N_2	–	233(−), 250(+), 300(−), 313(+), 330(+), 360(+)
	140–370		1	35.86 (36.70)		Loss of C_3H_3NO		
	370–700		1	56.96 (55.85)		Loss of C_7H_5O		
$[Cr(HL)_2(H_2O)_2]Cl_3{\cdot}H_2O$	35–110	61	1	14.62 (15.12)	87.76 (87.10)	Loss of H_2O and Cl_2	$½Cr_2O_3$	55(+), 160(+), 340(+), 455(−), 505(−), 700(+), 800(+).
	110–225	194	12	12.72 (12.15)		Loss of $2H_2O$ and $½Cl_2$		
	225–650	283, 449		60.42 (59.83)		Loss of 2L		
$[Mn(HL)_2(H_2O)_2]Cl_2{\cdot}4H_2O$	25–130	60	1	23.86 (24.03)	88.85 (88.24)	Loss of $4H_2O$ and Cl_2	MnO	40(−), 55(+), 100(−), 205(+), 312(−), 369(−), 549(−), 669(−), 712(−)
	130–750	548, 709	2	64.99 (64.21)		Loss of $2H_2O$ and 2L		
$[Fe(HL)_2(H_2O)_2]Cl_3{\cdot}2H_2O$	35–140	116	12	14.07 (14.82)	84.56 (84.61)	Loss of $2H_2O$, H_2O and HCl	$½Fe_2O_3$	60(−), 100(+), 255(+), 305(−), 365(−), 431(+), 530(−)
	140–650	288, 521		70.49 (69.79)		Loss of Cl_2 and 2L		
$[Co(HL)_2(H_2O)_2]Cl_2{\cdot}3H_2O$	25–115	73	1	9.27 (9.06)	80.49 (79.12)	Loss of $3H_2O$	CoO	50(−), 100(+), 120(−), 283(+), 350(+), 400(+), 460(−), 476(−), 575(−), 705(−)
	115–250	200	12	11.97 (11.99)		Loss of $2H_2O$ and $½Cl_2$		
	250–650	476, 557		59.25 (58.07)		Loss of $½Cl_2$ and 2L		
$[Ni(HL)_2(H_2O)_2]Cl_2{\cdot}4H_2O$	40–130	66	1	11.63 (11.72)	88.96 (87.79)	Loss of $4H_2O$	NiO	61(−), 215(+), 300(+), 399(−), 453(−), 605(−), 680(+)
	130–260	221	1	18.00 (17.42)		Loss of $2H_2O$ and Cl_2		
	260–700	391, 501, 580	3	59.33 (58.65)		Loss of 2L		
$[Cu(HL)_2(H_2O)_2]Cl_2$	25–130	150	1	6.38 (6.18)	85.48 (83.96)	Loss of $2H_2O$	CuO	65(+), 210(+), 290(−), 350(+), 397(+), 423(+), 486(+), 512(+), 575(−), 630(+), 650(−)
	130–230	303	13	16.72 (15.62)		Loss of 2HCl and H_2O		
	230–700	620		62.38 (62.16)		Loss of 2L		
$[Zn(HL)_2(H_2O)_2]\ Cl_2{\cdot}3H_2O$	25–85	52	1	9.46 (9.18)	85.87 (86.45)	Loss of $3H_2O$	ZnO	60(+), 150(+), 175(+), 340(+), 400(−), 450(−), 573(−), 608(−), 775(+), 810(−), 900(−)
	85–290	180	1	14.66 (15.47)		Loss of 2HCl and H_2O		
	290–950	606, 881	2	61.75 (61.80)		Loss of 2L		

+ endothermic; − exothermic

* Number of decomposition steps

value, confirming the covalent character of the metal–ligand bond. The axial symmetry parameter G value which was a measure of exchange coupling interaction between two metal ions was calculated for Cu(II) ions via the equation, $G = (g_{\|} - 2)/(g_{\perp} - 2)$ [43–45]. The calculated G value was higher than 4, suggesting a d_{x2-y2} ground state [43–45]. This result also indicated that the exchange coupling effects were not operative in the present complex [43–45].

Antimicrobial activity

The prepared ligand and its metal complexes were also tested for their antimicrobial activity, as illustrated in Table 5 and Fig. 1, against the following standard reference gram-positive (*Neisseria gonorrhoeae* and *Staphylococcus aureus*) and gram-negative (*Escherichia coli* and *Bacillus subtilis*) bacterial strains. Also, they are tested against *Candida albicans* fungus. The antimicrobial activity of the ligand and its metal complexes on both gram-positive and gram-negative bacteria and *Candida albicans* fungus was obtained by determining inhibitory zone diameter (mm mg^{-1} sample) as shown in Table 5 and Fig. 1. The chromene HL ligand is found to have no antimicrobial activity against *Neisseria gonorrhoeae*, *Bacillus subtilis* and *Candida albicans* organisms. In addition, Mn(II) complex has no antimicrobial activity against the organisms used in this study. It was obvious from Table 5 that Co(II) and Ni(II) complexes have antifungal activity similar to ketokonazole standard, while the others have no activity. The other metal complexes have antibacterial activity higher than the organisms used in this study and also the amikacin standard.

According to Tweedy's theory [46], it is found that chelation reduces the polarity of the metal atom due to its positive charge partially shared with a donor group and the possible π-electron delocalization over the whole chelate ring [47]. Therefore, the lipophilic character of the central metal atom could enhance such chelation, which subsequently favors its permeation through the lipid layers of the cell membrane and blocking the metal binding sites on enzymes of microorganism [46–48]. In addition, there are many factors which also increase the activity, namely solubility, conductivity and bond length between the metal and the ligand.

It is worth to mention that HL ligand showed similar or lower biological activity against the tested strains compared to the complexes. Structure activity relationships showed that $[Co(HL)_2(H_2O)_2]Cl_2{\cdot}3H_2O$, $[Cu(HL)_2(H_2O)_2]Cl_2{\cdot}3H_2O$ and $[Zn(HL)_2(H_2O)_2]Cl_2{\cdot}3H_2O$ complexes are of higher microbial activities [49, 50]. It may be due to the presence of two coumarin rings, which might increase the lipophilic character of the molecules, which facilitates the crossing through the biological membrane of the microorganisms and therefore inhibits their growth. The result revealed also that the complexes enhance the antimicrobial activity rather than the standard drugs [46–48].

Structural interpretation

Based on elemental analysis, 1:2 [metal]/[ligand] complexes were formed. IR spectral data revealed that the ligand behaves as neutral bidentate ligand, and octahedral geometry was proposed based on magnetic and reflectance spectra measurements. The complexes have molar conductance, and their thermal properties were studied. The structure of the complexes is given in Fig. 2.

Table 5 Biological activity of chromene ligand and its binary metal complexes

Sample	Inhibition zone diameter (mm mg^{-1} sample)				
	Escherichia coli	*Neisseria gonorrhoeae*	*Staphylococcus aureus*	*Bacillus subtilis*	*Candida albicans*
Control: DMSO	0.0	0.0	0.0	0.0	0.0
HL	10.0	0.0	10.0	0.0	0.0
$[Cr(HL)_2(H_2O)_2]Cl_3{\cdot}H_2O$	10.0	10.0	10.0	10.0	0.0
$[Mn(HL)_2(H_2O)_2]Cl_2{\cdot}4H_2O$	0.0	0.0	0.0	0.0	0.0
$[Fe(HL)_2(H_2O)_2]Cl_3{\cdot}2H_2O$	10.0	10.0	10.0	10.0	0.0
$[Co(HL)_2(H_2O)_2]Cl_2{\cdot}3H_2O$	13.0	10.0	10.0	10.0	9.0
$[Ni(HL)_2(H_2O)_2]Cl_2{\cdot}4H_2O$	10.0	10.0	10.0	10.0	10.0
$[Cu(HL)_2(H_2O)_2]Cl_2{\cdot}2H_2O$	12.0	12.0	12.0	12.0	0.0
$[Zn(HL)_2(H_2O)_2]\ Cl_2{\cdot}3H_2O$	10.0	10.0	13.0	10.0	0.0
Amikacin (antibacterial agent)	9.0	6.0	9.0	9.0	–
Ketokonazole (antifungal agent)	–	–	–	–	9

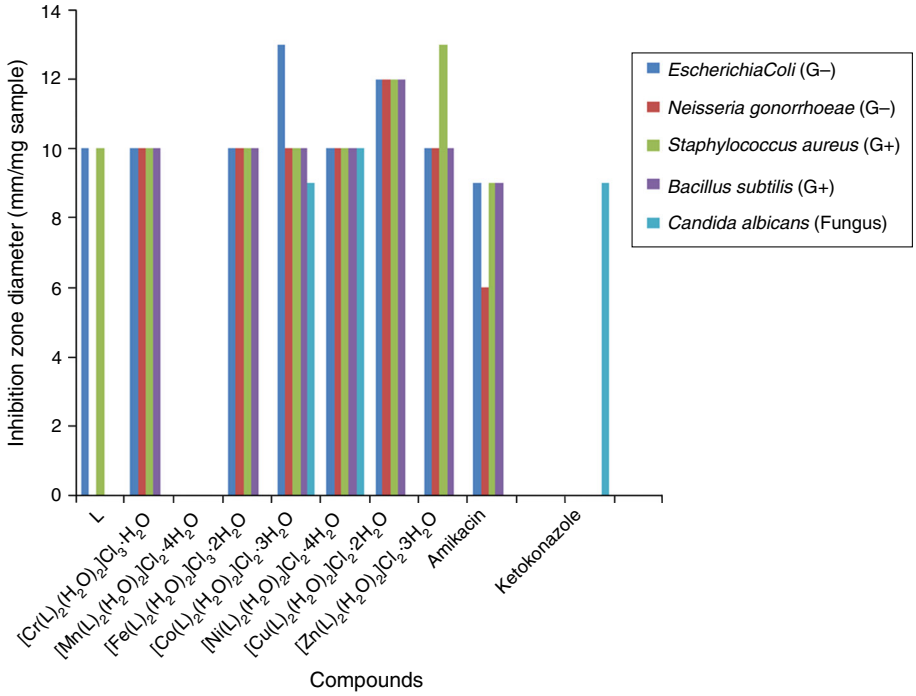

Fig. 1 Antimicrobial activity of chromene ligand, metal complexes and standards

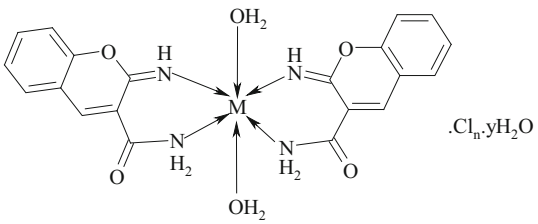

M = Cr(III) (y = 1); Fe(III) (y = 2); n = 3.
= Mn(II), Ni(II); n = 2; y = 4.
= Co(II), Zn(II); n = 2; y = 3.
= Cu(II); n = 2; y = 2.

Fig. 2 Structure of metal complexes

Conclusions

The investigated chromene ligand and its transition metal complexes were characterized based on different physico-chemical analysis. The complexes were isolated in 1:2 [M]/[L] ratio, have ionic nature and found to have octahedral structure. The thermal decomposition and the spectra of the complexes were fully characterized using elemental analysis, infrared, mass, electronic, ^{1}HNMR, electron spin resonance and magnetic studies. Infrared spectra discussed the chelation mode through the NH nitrogen and amino nitrogen without proton displacement. Structural activity relationships showed that $[Co(HL)_2(H_2O)_2]Cl_2{\cdot}3H_2O$, $[Cu(HL)_2(H_2O)_2]Cl_2{\cdot}3H_2O$ and $[Zn(HL)_2(H_2O)_2]Cl_2{\cdot}3H_2O$ complexes are of higher microbial activities. Co(II) and Ni(II) complexes have antifungal activity similar to ketokonazole standard, while the others have no activity. The other metal complexes have antibacterial activity higher than the amikacin standard.

Acknowledgements The authors wish to express their deep thank for Ms/Salma Ahmed for carrying out the biological activity study in this work.

References

1. El-Agrody AM, Abd El-Latif MS, El-Hady NA, Fakery AH, Bedair AH. Heteroaromatization with 4-hydroxycoumarin part II: synthesis of some new pyrano [2,3-d] pyrimidines, [1,2,4] triazolo [1,5-c] pyrimidines and pyrimido [1,6-b]-[1,2,4] triazine derivatives. Molecules. 2001;6:519–27.
2. Mazaahir K, Shilpi S, KhalilurRahman Khan M, Thukral SS. Aqua mediated synthesis of substituted 2-amino-4H-chromenes and in vitro study as antibacterial agents. Bioorg Med Chem Lett. 2005;15:4295–8.
3. El Azab IH, Abd El Latif FM. A simple and convenient synthesis of isolated-fused heterocycles based on: 2-imino-*N*-phenyl-2*H*-chromene-3-carboxamide. Open J Synth Theory Appl. 2012;1:44–57.
4. Andrea B, Nicole V, Jakob T, Sonja H, Stefan B, Christa EM. Synthesis and pharmacological evaluation of coumarin derivatives as cannabinoid receptor antagonists and inverse agonists. Bioorg Med Chem. 2009;17:2842–51.
5. Viselike P, Loannis KK, Panagiotis M, Nicole P, Loanna A. Synthesis and free radical scavenging activity of some new spiropyanocoumrins. Bioorg Med Chem Lett. 2008;18:5781–4.
6. Tadigoppula N, Tanvir K, Shweta N, Neena G, Suman G. Synthesis of chromenochalcones and evaluation of their in vitro antileishmanial activity. Bioorg Med Chem. 2005;13:6543–50.
7. William K, Shailaja K, Jiang SC, Zhang H, Zhao JH, Jia SJ, Xu LF, Crogan-Grundya C, Denis R, Barriault N, Vaillancourt L,

Charron S, Dodd J, Attardo G, Labrecque D, Lamothe S, Gourdeau H, Tseng B, Drewea J, Cai SX. Discovery of 4-aryl-4H-chromenes as a new series of apoptosis inducers using a cell-and caspase-based high-throughput screening assay. 2. Structure–activity relationships of the 7- and 5-, 6-, 8- positions. Bioorg Med Chem Lett. 2005;15:4745–51.
8. Djnielle G, Samuel V, Vijay LM, Frederic C, Guillaume V, Florence M, Philippe J, Rene G. The synthesis of new, selected analogues of the pro-apoptotic and anticancer molecule HA14-1. Tetrahedron Lett. 2008;49:3276–8.
9. Yuran L, Lin W, Chen B, Xie Y. Development of FRET-based ratiometric fluorescent Cu^{2+} chemodosimeters and the applications for living cell imaging. Org Lett. 2012;14:432–5.
10. Reddie KG, Humphries WH, Bain CP, Payne CK, Kemp ML, Murthy N. Fluorescent coumarinthiol measure biological redox couples. Org Lett. 2012;14:680–3.
11. Ali TE, Abdel-Aziz SA, El-Shaaer HM, Hanafy FI, El-Fauomy AZ. Synthesis of some new 4-oxo-4H-chromene derivatives bearing nitrogen heterocyclic systems an antifungal agents. Turk J Chem. 2008;32:365–74.
12. El-Ansary AL, Kandil AT, Issa YM, Soliman MH. Effect of some surface active substances on the spectrophotometric determination of Th(IV) using some coumarinazo dyes. Asian J Chem. 1998;10:86–98.
13. Issa YM, El-Ansary AL, Sayed SA, Soliman MH. Spectrophotometric determination of thulium (III) and dioxouranium ions using 8-(aryl azo)-6,7-dihydroxy-4-methyl coumarinderivatives. Egypt J Chem. 1999;42:37–47.
14. Katyal M, Singh HB. Analytical applications of hydroxycoumarins. Talanta. 1968;15:1043–5.
15. Omar MM. Studies on the dissociation constants of some substituted coumarinazo dyes in mixed solvents. Egypt J Chem. 1993;36:189–98.
16. Ligia RG, John NL, Femando C, Fernanda B. The crystal structures of four *N*-(4-halophenyl)-4-oxo-4H-chromene-3-carboxamides. Acta Crystallogr E CrystallogrCommun. 2015;71:88–93.
17. Kose D, Oztufk B, Sahin O, Buyukgungor O. Mixed ligand complexes of coumarilic acid/nicotinamide with transition metal complexes. J Therm Anal Calorim. 2014;115(1):515–1524.
18. Elgemeie GEH, Elghandour AHH. Activated nitriles in heterocyclic synthesis. Novel synthesis of 5-Imino-5H-[1] benzopyrano[3,4-c] pyridine-4(3H)-thiones and their oxo analogues. Bull Chem Soc Jpn. 1990;63:1230–2.
19. Lorian. Antibiotic in Laboratory Medicine. In: Einstein A, editor. Bronx, New York: College of Medicine; 1980. p. 176.
20. Boyd RF. General microbiology times mirror. Toro: Mosby Collage Publishing; 1984.
21. Irving H, Williams RJP. The stability of transition metal complexes. J Chem Soc. 1953;320:3192–210.
22. Jones RD, Summerville DA, Basolo F. Synthetic oxygen carriers related to biological systems. Chem Rev. 1979;79:139–79.
23. Mohamed GG, Soliman MH. Synthesis, spectroscopic and thermal characterization of sulpiride complexes of iron, manganese, copper, cobalt, nickel and zinc salts. Antibacterial and antifungal activity. Spectrochim Acta Part A. 2010;76:341–7.
24. Praveen Kumar S, Suresh R, Giribabu K, Manigandan R, Munusamy S, Muthamizh S, Narayanan V. Synthesis and characterization of chromium(III) Schiff base complexes: antimicrobial activity and its electrocatalytic sensing ability of catechol. Spectrochim Acta Part A. 2015;139:431–41.
25. Cotton FA, Wilkinson G, Murillo CA, Bochmann M. Advanced inorganic chemistry. 6th ed. New York: Wiley; 1999.
26. Mahmoud WH, Mohamed GG, El-Dessouky MMI. Coordination modes of bidentatelornoxicam drug with some transition metal ions. Synthesis, characterization and in vitro antimicrobial and antibreastic cancer activity studies. Spectrochim Acta A. 2014;122:598–608.
27. Soliman MH, Mohamed GG, Hindy AMM. Biological activity, spectral and thermal characterization of mixed ligand complexes of enrofloxacin and glycine: in vitro antibacterial and antifungal activity studies. Monatsh Chem. 2015;146:259–73.
28. Soliman MH, Hindy AMM, Mohamed GG. Thermal decomposition and biological activity studies of some transition metal complexes derived from mixed ligands sparfloxacin and glycine. Therm Anal Calorim. 2014;115:987–1001.
29. Mahmoud WH, Mohamed GG, El-Dessouky MMI. Synthesis, structural characterization, in vitro antimicrobial and anticancer activity studies of ternary metal complexes containing glycine amino acid and anti-inflammatory drug lornoxicam. Mol Struc. 2015;1082(1082):12–22.
30. Mohamed GG, Zayed MA, El-Gamel NEA. Preparation, chemical characterization and electronic spectra of 6-(2-pyridylazo)-3-acetamidophenol and its metal complexes. Spectrosc Lett. 2000;33:821–32.
31. Mahmoud WH, Mahmoud NF, Mohamed GG, El-Bindary AA, El-Sonbati AZ. Supramolecular structural, thermal properties and biological activity of 3-(2-methoxyphenoxy) propane-1,2-diol metal complexes. Mol Struc. 2015;1086:266–75.
32. Ali MA, Majumder SMMH, Butcher RJ, Jasinski JP, Jasinski JM. The preparation and characterization of bis-chelated nikel (II) complexes of the 6-methylpyridine-2-carboxaldehyde Schiff bases of S-alkyldithiocarbazates and the X-ray crystal structure of the bis {S-methyl-B-*N*-(6-methylpyrid-2-yl)-methylenedithiocarbazato}nickel(II) complex. Polyhedron. 1997;16:2749–54.
33. Zianna A, Ristović MS, Hatzidimitriou A, Papadopoulos CD, Kantouri ML. Synthesis, thermal analysis, and spectroscopic and structural characterizations of tetra nuclear nickel(II) cubane-type clusters with 2-hydroxybenzaldehydes or 2-hydroxyphenones. J Therm Anal Calorim. 2014;118(3):1431–40.
34. Mohamed GG, Nour EL-Dien FA, Khalil SM, Mohammad AS. Metal complexes of omeprazole. Preparation, spectroscopic and thermal characterization and biological activity. J Coord Chem. 2009;62:645–54.
35. Refat MS, Mohamed GG. Ti(IV), Cr(III), Mn(II) and Ni(II) complexes of the norfloxacin antibiotic drug: spectroscopic and thermal characterizations. J Chem Eng Data. 2010;55:3239–46.
36. Mahmoud WH, Mohamed GG, El-Dessouky MMI. Synthesis, characterization and in vitro biological activity of mixed transition metal complexes of lornoxicam with 1, 10-phenanthroline. Int J Electrochem Sci. 2014;9:1415–38.
37. Mohamed GG, Zayed EM, Hindy AMM. Coordination behavior of new bis Schiff base ligand derived from 2-furan carboxaldehyde and propane-1,3-diamine. Spectroscopic, thermal, anticancer and antibacterial activity studies. Spectrochim Acta A. 2015;145:76–84.
38. Lever ABP. Inorganic electronic spectroscopy. New York: Elsevier; 1968.
39. El-Sonbati AZ, Diab MA, El-Bindary AA, Mohamed GG, Morgan SM. Thermal, spectroscopic studies and hydrogen bonding in supra molecular assembly of azo rhodanine complexes. Inorg Chim Acta. 2015;430:96–107.
40. Dean JA. Langes hand book of chemistry. 14th ed. New York: McGraw-Hill; 1992.
41. Nakamoto K. Infrared spectra of inorganic and coordination compounds. New York: Wiley; 1970.
42. Ferraro JR. Low frequency vibrations of inorganic and coordination compounds. New York: Plenum Press; 1971.
43. Hathaway BJ, Billing DE. The electronic properties and stereochemistry of mono-nuclear complexes of the copper(II) ion. Coord Chem Rev. 1970;5:143–207.

44. Hathaway BJ. A new look at the stereochemistry and electronic properties of complexes of the copper (II) ion. Struct Bond. 1984;57:55–118.
45. Gudasi KB, Patil SA, Vadavi RS, Shenoy RV. Crystal structure of 2-[2-hydroxy-3-methoxyphenyl]-3-[2-hydroxy-3-methoxybenzylamino]-1,2dihydroquinazolin-4(3H)-one and the synthesis, spectral and thermal investigation of its transition metal complexes. Trans Met Chem. 2006;31:586–92.
46. Tweedy BG. Plant extracts with metal ions as potential antimicrobial agents. Phytopathology. 1964;55:910–4.
47. Singh Jadon SC, Gupta N, Singh RV. Synthetic and biochemical-studies of some hydrazine carbodithioic acid-derivatives of dioxomolybdenum(VI). Ind J Chem. 1995;34A:733–6.
48. Pelczar MJ, Chan ECS, Krieg NR. Microbiology. 5th ed. New York: McGraw-Hill; 1998.
49. Krajníková A, Rotaru A, Győryová K, Homzová K, Manolea HO, Kovářová J, Daniela Hudecová D. Thermal behaviour and antimicrobial assay of some new zinc(II) 2-aminobenzoate complex compounds with bioactive ligands. J Therm Anal Calorim. 2015;120(1):73–83.
50. Homzová K, Győryová K, Bujdošová Z, Hudecová D, Ganajová M, Vargová Z, Kovářová J. Synthesis, thermal, spectral and biological properties of zinc(II) 4-hydroxybenzoate complexes. J Therm Anal Calorim. 2014;116(1):77–91.